# Correlation of Car $S_1 \rightarrow$ Chl with Chl $\rightarrow$ Car $S_1$ Energy Transfer Supports the Excitonic Model in Quenched Light Harvesting Complex II

**Pen-Nan Liao,[†] Christoph-Peter Holleboom,[†] Laura Wilk,[‡] Werner Kühlbrandt,[‡] and Peter J. Walla*[,†,§]**

*Technische Universität Braunschweig, Institute for Physical and Theoretical Chemistry, Department for Biophysical Chemistry, Hans-Sommer-Strasse 10, 38106 Braunschweig, Germany, Max Planck Institute of Biophysics, Department of Structural Biology, Max-von-Laue-Strasse 3, 60438 Frankfurt am Main, Germany, and Max Planck Institute for Biophysical Chemistry, Department of Spectroscopy and Photochemical Kinetics, Am Fassberg 11, 37077 Göttingen, Germany*

*Received: April 16, 2010; Revised Manuscript Received: July 13, 2010*

Recently, excitonic carotenoid−chlorophyll interactions have been proposed as a simple but effective model for the down-regulation of photosynthesis in plants. The model was proposed on the basis of quenching-correlated electronic carotenoid−chlorophyll interactions (Car $S_1 \rightarrow$ Chl) determined by Car $S_1$ two-photon excitation and red-shifted absorption bands. However, if excitonic interactions are indeed responsible for this effect, a simultaneous correlation of quenching with increased energy transfer in the opposite direction, Chl $Q_y \rightarrow$ Car $S_1$, should be observed. Here we present a systematic study on the correlation of Car $S_1 \rightarrow$ Chl and Chl $\rightarrow$ Car $S_1$ energy transfer with the occurrence of red-shifted bands and quenching in isolated LHCII. We found a direct correlation between all four phenomena, supporting our conclusion that excitonic Car $S_1$−Chl interactions provide low-lying states serving as energy traps and dissipative valves for excess excitation energy.

## Introduction

Photosynthesis of higher plants starts from light harvesting by a series of light-harvesting complexes in the thylakoid membrane of chloroplasts. The absorbed solar light quanta are then transferred in a funnel-like manner with near 100% quantum efficiency to reaction centers where primary charge separation drives all subsequent biophysical and biochemical reactions. However, the light intensity in a typical day can suddenly increase by several orders of magnitude.[1] To prevent photo-oxidative damage to the reaction center and other parts of the photosynthetic apparatus in this situation, they have evolved a photoprotective mechanism which down-regulates the light-harvesting antenna to a state in which excess energy is dissipated harmlessly as heat. This mechanism is often referred to as nonphotochemical quenching (NPQ). In higher plants the major component of nonphotochemical quenching is energy-dependent quenching (qE).[2,3] It is known that qE is a fast reversible process and depends on the *trans*-thylakoid pH gradient ($\Delta$pH),[2,4] the presence of the protein PsbS,[5] and the xanthophyll cycle carotenoid zeaxanthin (Zea).[3] Although many studies have aimed at unravelling the quenching mechanism and several different regulation models have been proposed, a fundamental understanding is still missing.[5−10]

The most abundant antenna complex in higher plants is light harvesting complex II (LHCII). In recent crystal structures, chromophores in each LHCII monomer can be clearly distinguished as 8 Chlorophyll a (Chl a), 6 Chlorophyll b (Chl b), and 4 carotenoid molecules.[11,12] More than half of the light energy used for higher plant photosynthesis is collected by the chromophores in this protein complex. Several studies suggest that, apart from light harvesting and energy transfer, LHCII plays a key role in the regulation of qE by switching it into a quenched state due to mechanisms that are so far not completely understood.[6,13] In these studies it has been proposed that interactions between carotenoids and chlorophylls may create dissipation valves for excess excitation energy.[7,14] Other studies have presented evidence for minor antennae complexes as main regulators.[15,16] In our previously reported experiments, we have shown that the chlorophyll fluorescence quenching and photosynthetic down-regulation in LHCII and entire plants correlate linearly with the electronic coupling between carotenoid $S_1$ and chlorophyll.[14,17,18] In addition, red-shifted absorption bands were observed in quenched LHCII.[14,19] On the basis of these observations and other findings,[7,20] we proposed a quenching model in which excitonic interactions between carotenoids and chlorophylls are formed.[21] This would easily explain quenching in the antenna by the following simple mechanism: First, excitonic interactions always lead to low-lying excitonic states that act automatically as energy traps for the entire pigment pool. Second, these excitonic states should have significantly shorter excited state lifetimes than pure chlorophyll states (a few nanoseconds) due to the short-lived character of the participating carotenoid dark states (10−30 ps). As a result, excess excitation energy from these states is quickly dissipated as heat.

The carotenoid−chlorophyll interactions that were correlated with the quenching were determined by two-photon spectroscopy. Using the two-photon technique, carotenoids in LHCII and intact plants can be selectively excited from the ground state (Car $S_0$) to the first excited state (Car $S_1$).[22−25] A subsequent occurrence of chlorophyll fluorescence provides direct evidence for energy flow from Car $S_1$ to the Chl $Q_y$ state. In our previous work, we observed a simultaneously increased energy transfer in the direction Car $S_1 \rightarrow$ Chl $Q_y$ in down-regulated living plants as well as in aggregated LHCII.[14,17] Energy transfer and excitonic interactions are both governed by the same electronic

* Corresponding author. E-mail: pwalla@gwdg.de.
[†] Technische Universität Braunschweig.
[‡] Max Planck Institute of Biophysics.
[§] Max Planck Institute for Biophysical Chemistry.

10.1021/jp1034163 
Published on Web 11/09/2010

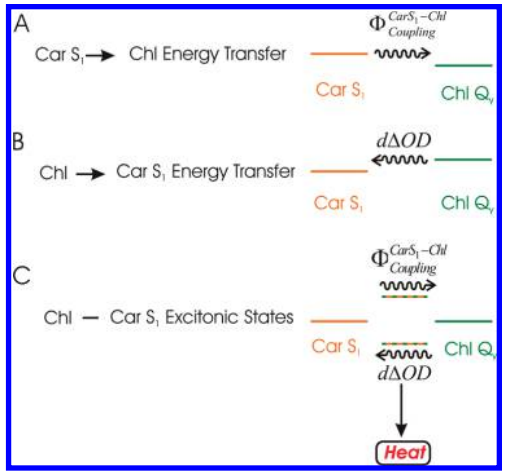


**Figure 1.** If electronic coupling is present between two pigments A and B, it depends only on the relative state energy whether (a) A→B energy transfer, (b) B→A energy transfer, or (c) excitonic A−B mixing occurs. In the latter case, excitation of either A or B will result in a simultaneous excitation of B or A, respectively, that clearly indicates the presence of excitonic mixing.

interactions. If the energies of both participating pigments are significantly different, then electronic interactions lead to energy transfer to the energetically lower state, i.e., either in the direction Car $S_1 \rightarrow$ Chl $Q_y$ (Figure 1 A) or in the direction Chl $\rightarrow$ Car $S_1$ (Figure 1 B). Only when the energies of the participating molecules are similar, excitonic interactions are formed with the consequence that an excitation of either pigment results in a transfer of energy to the other pigment, respectively (Figure 1 C). If indeed excitonic interactions occur between the two types of pigments, a correlated increase in the energy flow should be observable in both directions as both molecules share excitation energy. It should be noted that a simultaneous increase of energy flow in both directions can also be obtained due to increasing heterogeneities of the sample, i.e., the energy level distribution in either or both Car or Chl. Depending on the time scales and amplitudes of the change in energy levels, individual chlorophyll−carotenoid pairs then contribute more or less often to excitonic interactions.

To provide additional evidence in favor of or against the excitonic quenching model, we present here a systematic study on correlations between Car $S_1 \rightarrow$ Chl as well as Chl $\rightarrow$ Car $S_1$ energy transfer with fluorescence quenching in isolated LHCII and the occurrence of red-shifted absorption bands. The energy flow in the direction Car $S_1 \rightarrow$ Chl was monitored using our two-photon technique. Simultaneously, the energy flow in the opposite direction, Chl $Q_y \rightarrow$ Car $S_1$, was observed by detecting the strong Car $S_1 \rightarrow$ Car $S_n$ transient absorption after direct Chl excitation.[7,20] The fluorescence quenching and the occurrence of red-shifted absorption bands was monitored using conventional fluorescence and absorption spectrometry. Indeed, we found a direct correlation between all four parameters. The observation that in quenched samples a bidirectional increase in the energy transfer, Car $S_1 \rightarrow$ Chl and Chl $\rightarrow$ Car $S_1$, occurs that correlates directly with red-shifted absorption bands supports the hypothesis that in these samples indeed excitonic interactions between carotenoids and chlorophylls are present.

## Materials and Methods

**Sample Preparation.** Native LHCII proteins were isolated from spinach as described previously.[26] LHCII suspended in buffer solution (Tris, pH 7.5, 0.3% *n*-nonyl-$\beta$-D-glucopyranoside) was incubated in a cuvette with SM-2 absorbent (Bio-Rad). The PAM fluorometer was used to measure the chlorophyll fluorescence during the incubation. A range of differently quenched, aggregated LHCII samples were obtained after different incubation times. The concentration of LHCII was adjusted to OD of ~0.3/mm at 673 nm. Absorption and fluorescence spectra of LHCII were recorded on a Lambda 25 UV/vis spectrometer from Perkin-Elmer and a Cary Eclipse fluorescence spectrophotometer from Varian, respectively.

**Two-Photon Spectroscopy.** The laser system consisted of a Vitesse Duo and a RegA 9000 pumped optical parametric amplifier OPA 9450 (all components from Coherent Inc.). The system was set at a repetition rate of 120 kHz. The OPA provided pulses of about 120 fs fwhm. For two-photon excitation of carotenoids, the idler beam was tuned to 1188 nm. A hot mirror (L46-386, Edmund Optics) and a 1100 nm long pass filter (FEL1100 nm, Thorlabs) were used to thoroughly reject the visible light of the signal beam to prevent any undesired chlorophyll one-photon excitation. The idler beam was focused at LHCII samples, and the emitted chlorophyll fluorescence was collected with a confocal setup. The chlorophyll fluorescence upon two-photon excitation was detected by a fast photodiode (designed by Prof. D. Schwarzer) which was connected to a lock-in amplifier (EG&G 5205, Dumberry, Canada) synchronized with a mechanical chopper positioned in the idler beam. For one-photon excitation, a conventional PAM fluorometer (FMS1, Hansatech) integrated into the confocal setup was used. The modulating beam of 594 nm from the PAM fluorometer was used to perform one-photon excitation. The chlorophyll fluorescence upon one-photon excitation was detected by the PAM fluorometer.

**Transient Absorption Spectroscopy.** For the TA experiments, the pump pulses were tuned to 673 and 654 nm. The pump energy per pulse was about 8−14 nJ. The pump beam was sent through a delay stage (M-ILS 200 CCH A with controller MM4005, Newport GmbH, Darmstadt, Germany) to vary the time delay between the pump and probe pulses. For probe pulses, a part of the white light continuum of the OPA was used. The desired wavelength of the probe beam was selected by a gradient interference filter mounted on a translation stage. The pump and probe pulses were focused into the sample with achromatic lenses ($f = 5$ and $f = 10$ cm, respectively) mounted to three-dimensional translation stages. A sample cell with a path length of 1 mm was used. The sample solution was pumped to flow back and forth by a peristaltic pump (400FD/A1, Watson-Marlow GmbH, Rommerskirchen, Germany) and chilled by a circulating water bath (RC-20 S, LAUDA, Lauda-Königshofen, Germany) which was set at 4 °C to prevent sample degradation during the data acquisition. After passing through the cell, the probe beam was focused into a monochromator (Chromex, 500IS/SM, Bruker Optics, Ettlingen, Germany). The TA signal was detected by the home-built fast photodiode which was connected to the lock-in amplifier. The lock-in amplifier was again synchronized with a chopper which was positioned in the pump beam path. All experimental parameters used for the determination of transient absorption kinetics are essentially identical to the setup used by Ma et al.[20] to determine transient absorption kinetics in thylakoid membranes. The per pulse excitation energy we used in the present work was about two to three times smaller than the energies used in that study. It has been shown that such excitation intensities avoid annihilation in LHCII[27] and even in very large pigment−protein complexes like PS I.[28]

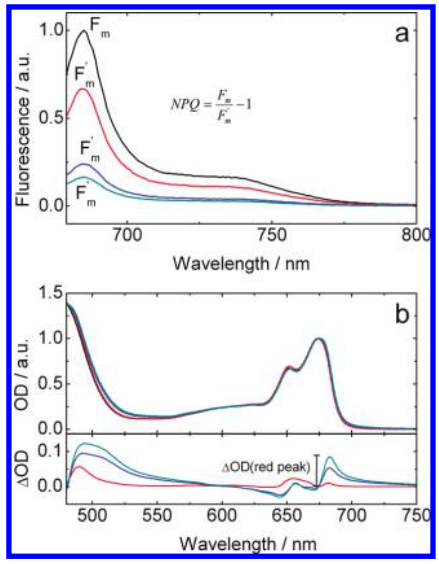


**Figure 2.** (a) Fluorescence spectra of different LHCII oligomerization states and (b) their corresponding absorption spectra and absorption difference spectra.

## Results and Discussion

First, we repeated the measurement of electronic couplings between carotenoids and chlorophylls as a function of fluorescence quenching in LHCII as in our previous study.[17] The detection of fluorescence from the Chl a $Q_y$ states upon selective two-photon excitation ($Fl^{TPE}$) of the carotenoid dark states, Car $S_1$, provides direct evidence for electronic interactions between Car $S_1$ and Chl $Q_y$ states. Therefore, this experiment reflects the energy flow in the direction Car $S_1 \rightarrow$ Chl a. A quantitative comparison of the Chl fluorescence intensity detected upon selective excitation of the carotenoid dark states, $Fl^{TPE}$, and direct one-photon excitation of the Chl, $Fl^{OPE}$, allows quantification of the current extent of these interactions, $\phi^{CarS_1-Chl}_{Coupling}$ (more details about this coupling parameter are described in our previous study[14])

$$\Phi^{CarS_1-Chl}_{Coupling} \propto \frac{Fl^{TPE}}{Fl^{OPE}} \quad (1)$$

The quenching of the aggregated LHCII was quantified from the maximum fluorescence of unquenched LHCII detected at 685 nm, $F_m$, and the fluorescence intensities of quenched LHCII at the same wavelength, $F_m'$

$$NPQ = \frac{F_m}{F_m'} - 1 \quad (2)$$

A range of quenched states of isolated LHCII was prepared, which covers a 5-fold difference in fluorescence quantum yield (Figure 2a). Quenching was induced by aggregation of LHCII using SM-2 absorbent. Figure 3 shows that we observed the same linear correlation between $\phi^{CarS_1-Chl}_{Coupling}$ and NPQ as in our previous report.[17]

In Figure 2b, the corresponding absorption spectra of LHCII in different quenched states are shown along with the corresponding absorption difference spectra calculated by subtracting the spectrum of the unquenched LHCII from the spectra of the quenched LHCII samples. In the absorption difference spectra, the same red-shifted bands are observed as described previously.[14,17,19]

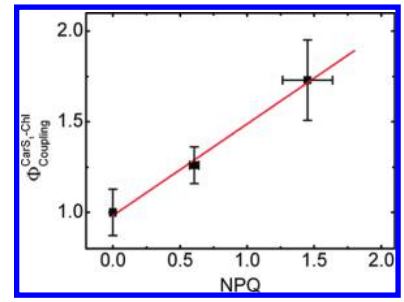


**Figure 3.** Correlation between $\phi^{CarS_1-Chl}_{Coupling}$ and fluorescence quenching, NPQ.

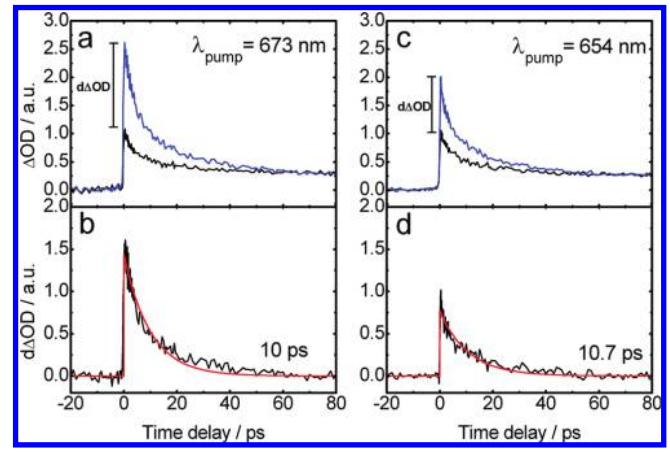


**Figure 4.** (a and c) Transient absorption kinetics of unquenched (black line) and quenched (blue line) LHCII after excitation at 673 and 654 nm, respectively. The maximum amplitudes of the unquenched profiles were normalized to 1. (b and d) The difference between quenched and unquenched kinetics in a and c. The monoexponential fits (red line) are shown with their corresponding decay lifetimes.

The bands arise at ~681 ± 1 nm and progressively increase in intensity with the extent of quenching. This band is shifted about ~130 ± 20 $cm^{-1}$ to the red in comparison to the main chlorophyll a peak at ~675 ± 1 nm. Within the experimental uncertainties, this red-shift is very close to the value of ~80 $cm^{-1}$ that has been reported by Ilioaia et al. for the shift in the short-living component (~40 ps) of the chlorophyll fluorescence in quenched LHCII samples.[29] It is generally assumed that only one or a few chlorophylls are participating in the formation of quenching interactions, and so it is not surprising that only a minor fraction of the chlorophyll absorption shows a red shift. The magnitude of the red-shifted peak in the most quenched sample is ~10% of the magnitude of the main chlorophyll a $Q_y$ peak at ~675 nm. This magnitude indicates that at least one or even only one chlorophyll out of the 8 LHCII chlorophyll a molecules is participating in the observed effects (1/8 = 12.5%).

In addition, we performed TA measurements on quenched and unquenched LHCII to determine the energy transfer in the opposite direction, Chl $\rightarrow$ Car $S_1$. The samples were excited at 673 nm, corresponding to the absorption maximum of the Chl $Q_y$ band. As the probe wavelength, 510−590 nm was chosen which corresponds to the $S_1 \rightarrow S_n$ transition band of carotenoids. A multiexponential global analysis of the decay kinetics shown in Figure 4a shows that the decay kinetics of aggregated LHCII is essentially the same as those presented in the detailed transient absorption study of Müller et al.[28] Upon close inspection of the kinetic traces, the decays at longer delay time (>~60 ps) are kinetically indistinguishable. Therefore, we rescaled the kinetic data in the same way as described in Ma et al. for intact thylakoid membranes so they would match each other at longer

delay times.[20] The scaling usually did not result in amplitude differences larger than 10−20%. These differences are most likely a consequence of slightly different sample concentrations and pump/probe alignments. Resulting kinetics, in which the probe wavelength was set at 540 nm, are shown in Figure 4a. The transient absorption amplitude under quenched conditions is two times higher than that for unquenched conditions. As compared with the quenched states of thylakoid membranes, the magnitude of the additional signal in quenched LHCII is significantly larger.[20] The transient signal of quenched LHCII originates from carotenoid excited state absorption (ESA) as a $S_1 \rightarrow S_n$ transition, together with the contribution of Chl ESA. Under unquenched conditions, the signal is dominated by Chl ESA.[20] To extract the additional signals contributed from carotenoids under quenched conditions, we subtracted the data of unquenched LHCII from the data of quenched LHCII, as previously described by Ma et al.[20] The corresponding difference curve (d$\Delta$OD) is shown in Figure 4b. The difference data indicate an additional Car $S_1$ population after exciting Chl for the quenched samples. A fit of a monoexponential decay function to the difference profile yields a decay time of 10 ps. This decay time is nearly identical to the decay time of 9.9 ps observed by Ma et al. for intact thylakoid membranes, where the quenched state was induced by high light illumination.[20] No rise can be detected in the data within the time resolution of our apparatus (~90 fs fwhm). This instantaneous occurrence of a signal in the spectral Car $S_1$ transient absorption region after Chl excitation provides another important piece of indication for excitonic interactions. If the states of these two pigments mix excitonically, then Car $S_1$ is also instantaneously excited when Chl is excited. If only energy transfer would occur between these states, then at least some rise kinetic should be observable except in the case of extremely fast energy transfer. Figure 4c shows corresponding data of an experiment using a pump beam wavelength which is blue-shifted to 654 nm. A pump wavelength of 654 nm corresponds to the blue edge of the Chl $Q_y$ band and is reported to have a larger magnitude in the kinetic differences between the quenched and unquenched states of thylakoid membranes.[20] However, for LHCII we observed less difference using the blue-shifted pump beam (Figure 4c). The amplitude of the quenched sample is 2.5 times higher for 673 nm excitation but only 1.8 times higher for 654 nm excitation. A decay lifetime of 10.7 ps is obtained for the difference kinetics (Figure 4d).

To demonstrate that the kinetic difference data predominantly represent Car $S_1$ transient absorption, we constructed a spectrum of the difference signals for various wavelengths. A global lifetime analysis was chosen to extract the time constant associated with the additional signal in the quenched LHCII. In the fit, the lifetimes were forced to be identical for all wavelengths, and the amplitudes were fitted freely for each different wavelength. In this global analysis a decay lifetime of 13.5 ps was obtained, and the resulting amplitudes of the difference kinetic profiles are plotted in Figure 5. With a maximum at ~530 nm, this spectrum is very similar to the spectrum recorded by Ma et al. using intact thylakoid membranes.[20] We compared this reconstructed spectrum with the Car $S_1$ transient absorption spectrum measured by Polivka and co-workers (dashed line in Figure 5) using native LHCII recorded 6 ps after excitation at 510 nm, when the internal conversion Car $S_2$−Car $S_1$ is virtually completed.[30] Both spectra are in good agreement within the experimental noise. The differences and accuracy in the lifetime determined for a single wavelength (Figure 3b and d) or in a global analysis are comparable to or smaller than differing kinetic values reported for quenched LHCII in the literature.[7,28]

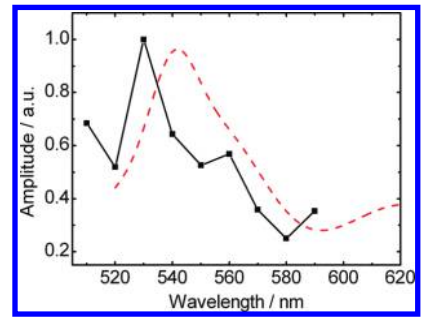


**Figure 5.** Reconstructed spectrum of difference kinetics between quenched and unquenched LHCII probed at 510−590 nm (solid line). The dashed line shows the Car $S_1$ TA spectrum determined by Polivka and co-workers using native LHCII, which was taken 6 ps after excitation at 510 nm.[30]

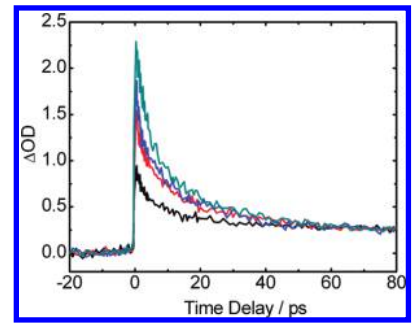


**Figure 6.** Transient absorption kinetics of different quenched states of LHCII probed at 540 nm upon 673 nm chlorophyll excitation. The black line shows the kinetics of unquenched LHCII. The red, blue, and cyan lines show the kinetics of quenched LHCII with progressively increased chlorophyll fluorescence quenching, NPQ, respectively.

In a next step, we determined the magnitude of difference kinetics between quenched and unquenched samples as a function of the extent in quenching. These measurements were performed using a probe wavelength of 540 nm and a chlorophyll excitation wavelength of 673 nm. The corresponding data (Figure 6) show that there is a correlation between the magnitude of Car $S_1$ excitation upon Chl excitation and the extent in fluorescence quenching. The TA amplitude is progressively increasing with the extent of aggregation-dependent quenching in LHCII. This finding confirms that an increase of energy flow from chlorophylls to carotenoids takes place and results in an increasingly higher population of Car $S_1$ with the extent of fluorescence quenching in LHCII.

Figure 7 summarizes the correlation between all four parameters determined in this work: the Car $S_1 \rightarrow$ Chl energy transfer as quantified by $\phi_{\text{Coupling}}^{\text{CarS}_1-\text{Chl}}$ (Figure 3) as well as the Chl $\rightarrow$ Car $S_1$ energy transfer, as quantified by the difference amplitudes in the kinetic traces, d$\Delta$OD (Figure 6 and Figure 4), the occurrence of red-shifted absorption bands as quantified by the optical density in the difference absorption spectra, $\Delta$OD (red peak) (Figure 2b), and the quenching of the LHCII as quantified by the parameter NPQ (Figure 2a).

In Figure 7a, the correlation between $\phi_{\text{Coupling}}^{\text{CarS}_1-\text{Chl}}$ and NPQ and in Figure 7b the correlation between the red peak intensity, $\Delta$OD (red peak), and NPQ are shown. Figure 7c shows that there consequently also exists a linear correlation between the red peaks, $\Delta$OD (red peak), and the Car $S_1 \rightarrow$ Chl energy flow, $\phi_{\text{Coupling}}^{\text{CarS}_1-\text{Chl}}$.

Figure 7d shows that also the energy flow in the direction Chl $\rightarrow$ Car $S_1$, determined by the additional, Car $S_1$ transient

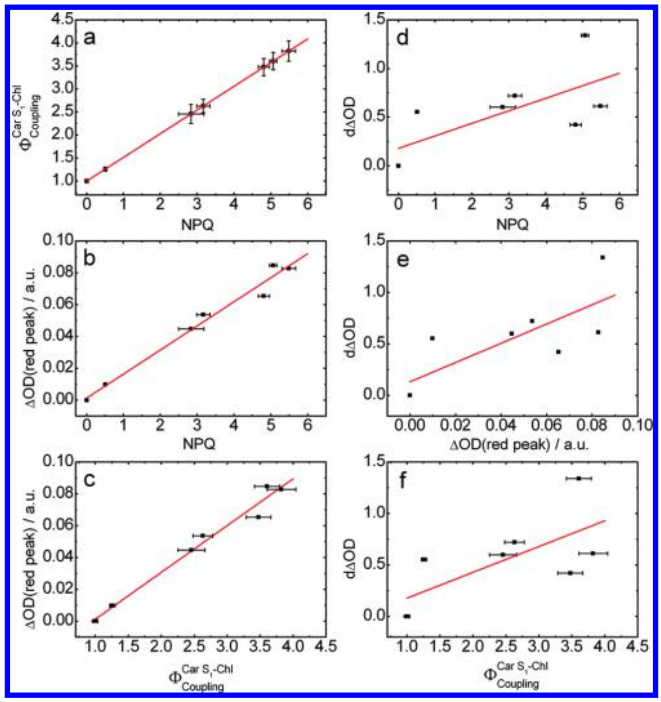


**Figure 7.** (a) Correlation between $\phi_{\text{Coupling}}^{\text{CarS}_1-\text{Chl}}$ and fluorescence quenching, NPQ. (b) Correlation between the red peak intensity, ΔOD (red peak), and fluorescence quenching, NPQ. (c) Correlation between the red peak intensity, ΔOD (red peak), and $\phi_{\text{Coupling}}^{\text{CarS}_1-\text{Chl}}$. (d) Correlation between dΔOD, reflecting Chl → Car $S_1$ energy transfer, and fluorescence quenching, NPQ. (e) Correlation between dΔOD and the red peak intensity, ΔOD (red peak). (f) Correlation between dΔOD and $\phi_{\text{Coupling}}^{\text{CarS}_1-\text{Chl}}$.

absorption signal, is linearly correlated to the fluorescence quenching, NPQ. Since it is harder to obtain quantitatively transient absorption signals, this correlation is more noisy, but it represents important, additional evidence that indeed excitonic mixing is responsible for all observed effects. These data show that the quenching is correlated to increased energy flow not only in the Car $S_1$ → Chl direction but also in both directions, Car $S_1$ → Chl and Chl → Car $S_1$, which is only possible when the molecules actually share energy by excitonic interactions (Figure 1C). Therefore, it is not surprising that this instantaneous Chl → Car $S_1$ energy transfer also correlates linearly with the occurrence of red-shifted absorption bands (Figure 7e) and $\phi_{\text{Coupling}}^{\text{CarS}_1-\text{Chl}}$ (Figure 7f).

## Conclusions

Figure 7 shows that all of the following four parameters are directly and positively correlated to each other. The four parameters are (1) $\phi_{\text{Coupling}}^{\text{CarS}_1-\text{Chl}}$ determined by two-photon spectroscopy and reflecting Car $S_1$ → Chl energy transfer, (2) dΔOD determined by transient absorption spectroscopy and reflecting Chl → Car $S_1$ energy transfer, (3) ΔOD (red peak) reflecting additional red-shifted bands in the absorption spectra, and (4) NPQ reflecting the fluorescence quenching. We conclude that in quenched LHCII excitation of Car $S_1$ always leads to an excitation of Chl and simultaneously that excitation of Chl also always leads to an excitation of Car $S_1$. In addition, the Car $S_1$ signals occur instantaneously with Chl excitation in the quenched state, and red-shifted bands are formed that correlate with all other effects. This is exactly what is expected when both states, Car $S_1$ and Chl, mix excitonically. The observation that in quenched samples a bidirectional increase in energy transfer, Car $S_1$ → Chl and Chl → Car $S_1$, occurs that correlates directly with red-shifted absorption bands is in strong support of our hypothesis that indeed excitonic interactions between carotenoids and chlorophylls are present, resulting in low-lying states serving as energy traps and dissipative valves for excess excitation energy (Figure 1). The red-shifted bands in the absorption spectra are also a typical indicator of excitonic interactions since new, lower energetic states are formed. Similar red-shifted bands have also been observed in the LHCII fluorescence by others.[19]

Excitonic Car $S_1$−Chl interactions will automatically lead to very effective quenching centers as they form energetically low trapping states that have a very short lifetime due to the short-lived Car $S_1$ contribution. Recently, it has been suggested that the quenching interactions are caused by Chl−Chl interactions.[28] It is certainly possible that both occur, increasing Chl−Chl as well as increasing Car−Chl interactions in the quenched state. For example, several chlorophylls are already subject to stronger electronic interactions in the unquenched state and are therefore already dominant local energy traps.[6,18,31] If these chlorophylls interact in addition with carotenoids, electronic interactions including several chlorophyll molecules as well as carotenoids would generate an effective dissipation valve for excess excitation energy.

**Acknowledgment.** This work was supported by the Fonds der Chemischen Industrie and the Deutsche Forschungsgemeinschaft (DFG).

## References and Notes

(1) Demmig-Adams, B.; Adams, W. W. *Science* **2002**, *298*, 2149.
(2) Horton, P.; Ruban, A. V.; Walters, R. G. *Annu. Rev. Plant Physiol. Plant Mol. Biol.* **1996**, *47*, 655.
(3) Müller, P.; Li, X.-P.; Niyogi, K. K. *Plant Physiol.* **2001**, *125*, 1558.
(4) Krause, G. H.; Weis, E. *Annu. Rev. Plant Physiol. Mol. Biol.* **1991**, *42*, 313.
(5) Li, X. P.; Björkman, O.; Shih, C.; Grossman, A. R.; Rosenquist, M.; Jansson, S.; Niyogi, K. K. *Nature* **2000**, *403*, 391–395.
(6) Pascal, A. A.; Liu, Z.; Broess, K.; Oort, B. v.; Amerongen, H. v.; Wang, C.; Horton, P.; Robert, B.; Chang, W.; Ruban, A. *Nature* **2005**, *436*, 134.
(7) Ruban, A. V.; Berera, R.; Ilioaia, C.; van Stokkum, I. H. M.; Kennis, J. T. M.; Pascal, A. A.; van Amerongen, H.; Horton, P.; van Grondelle, R. *Nature* **2007**, *450*, 575.
(8) Frank, H. A.; Bautista, J. A.; Josue, J. S.; Young, A. J. *Biochemistry* **2000**, *39*, 2831.
(9) Holt, N. E.; Zigmantas, D.; Valkunas, L.; Li, X.-P.; Niyogi, K. K.; Fleming, G. R. *Science* **2005**, *307*, 433.
(10) Ahn, T. K.; Avenson, T. J.; Ballottari, M.; Cheng, Y.-C.; Niyogi, K. K.; Bassi, R.; Fleming, G. R. *Science* **2008**, *320*, 794.
(11) Liu, Z.; Wang, K.; Kuang, T.; Zhang, J.; Gui, L.; An, X.; Chang, W. *Nature* **2004**, *428*, 287.
(12) Standfuss, J.; van, A. C. T.; Scheltinga; Lamborghini, M.; Kühlbrandt, W. *EMBO J.* **2005**, *24*, 919.
(13) Horton, P.; Johnson, M. P.; Perez-Bueno, M. L.; Kiss, A. Z.; Ruban, A. V. *FEBS Lett.* **2008**, *275*, 1069.
(14) Bode, S.; Quentmeier, C. C.; Liao, P.-N.; Hafi, N.; Barros, T.; Wilk, L.; Bittner, F.; Walla, P. J. *Proc. Natl. Acad. Sci. U.S.A.* **2009**, *106*, 12311.
(15) Mozzo, M.; Passarini, F.; Bassi, R.; van Amerongen, H.; Croce, R. *Biochim. Biophys. Acta* **2008**, *1777*, 1263.
(16) Avenson, T. J.; Ahn, T. K.; Zigmantas, D.; Niyogi, K. K.; Li, Z.; Ballottari, M.; Bassi, R.; Fleming, G. R. *J. Biol. Chem.* **2008**, *283*, 3550.
(17) Liao, P.-N.; Bode, S.; Wilk, L.; Hafi, N.; Walla, P. J. *Chem. Phys.* **2010**, in press.
(18) Frähmcke, J. S.; Walla, P. J. *Chem. Phys. Lett.* **2006**, *430*, 397.
(19) Ruban, A. V.; Horton, P. *Biochim. Biophys. Acta* **1992**, *1102*, 30.
(20) Ma, Y. Z.; Holt, N. E.; Li, X. P.; Niyogi, K. K.; Fleming, G. R. *Proc. Natl. Acad. Sci. U.S.A.* **2003**, *100*, 4377.
(21) van Amerongen, H.; van Grondelle, R. *J. Phys. Chem. B* **2001**, *105*, 604.
(22) Bode, S.; Quentmeier, C. C.; Liao, P.-N.; Barros, T.; Walla, P. J. *Chem. Phys. Lett.* **2007**, *450*, 379.
(23) Wehling, A.; Walla, P. J. *Photosynth. Res.* **2006**, *90*, 101.
(24) Hilbert, M.; Wehling, A.; Schlodder, E.; Walla, P. J. *J. Phys. Chem. B* **2004**, *108*, 13022.
(25) Wehling, A.; Walla, P. J. *J. Phys Chem. B* **2005**, *109*, 24510.
(26) Kühlbrandt, W.; Thaler, T.; Wehrli, E. *J. Cell. Biol.* **1983**, *96*, 1414.

(27) Barzda, V.; Gulbinas, V.; Kananavicius, R.; Cervinskas, V.; van Amerongen, H.; van Grondelle, R.; Valkunas, L. *Biophys. J.* **2001**, *80*, 2409.

(28) Müller, M. G.; Lambrev, P.; Reus, M.; Wientjes, E.; Croce, R.; Holzwarth, A. R. *ChemPhysChem* **2010**, *11*, 1289.

(29) Ilioaia, C.; Johnson, M. P.; Horton, P.; Ruban, A. V. *J. Biol. Chem.* **2008**, *283*, 29505.

(30) Polívka, T.; Zigmantas, D.; Sundström, V.; Formaggio, E.; Cinque, G.; Bassi, R. *Biochemistry* **2002**, *41*, 439.

(31) van Grondelle, R.; Novoderezhkin, V. I. *Phys. Chem. Chem. Phys.* **2006**, *8*, 793.

JP1034163